

PIGEON: Optimizing CUDA Code Generator for End-to-End Training and Inference of Relational Graph Neural Networks

Kun Wu
University of Illinois
at Urbana-Champaign*

Mert Hidayetoğlu
Stanford University

Xiang Song
AWS AI Research
and Education

Sitao Huang
University of California,
Irvine

Da Zheng
AWS AI Research
and Education

Israt Nisa
AWS AI Research
and Education

Wen-mei Hwu
University of Illinois
at Urbana-Champaign

Abstract

Relational graph neural networks (RGNNs) are graph neural networks (GNNs) with dedicated structures for modeling the different types of nodes and/or edges in heterogeneous graphs. While RGNNs have been increasingly adopted in many real-world applications due to their versatility and accuracy, they pose performance and system design challenges due to their inherent computation patterns, gap between the programming interface and kernel APIs, and heavy programming efforts in optimizing kernels caused by their coupling with data layout and heterogeneity. To systematically address these challenges, we propose Pigeon, a novel two-level intermediate representation (IR) and its code generator framework, that (a) represents the key properties of the RGNN models to *bridge the gap* between the programming interface and kernel APIs, (b) *decouples* model semantics, data layout, and operators-specific optimization from each other to reduce programming efforts, (c) *expresses and leverages* optimization opportunities in inter-operator transforms, data layout, and operator-specific schedules. By building on one general matrix multiply (GEMM) template and a node/edge traversal template, Pigeon achieves up to $7.8\times$ speed-up in inference and $5.6\times$ speed-up in training compared with the state-of-the-art public systems in select models, i.e., RGCN, RGAT, HGT, when running heterogeneous graphs provided by Deep Graph Library (DGL) and Open Graph Benchmark (OGB). Pigeon also triggers fewer out-of-memory (OOM) errors. In addition, we propose linear operator fusion and compact materialization to further accelerate the system by up to $2.2\times$.

1 Introduction

Graph neural networks (GNNs) have been increasingly deployed in real-world applications, including fraud detection, recommendation, and social networks. In response to this growing demand, the open source community has made many

efforts to provide GNN-specific machine learning frameworks, such as Deep Graph Library (DGL) [28] and PyTorch Geometric (PyG) [7]. These frameworks implement several highly optimized operations, including sparse-dense matrix multiplication (SpMM) and sampled dense-dense matrix multiplication (SDDMM) to speed up message passing operations [12]. Most of these optimizations have focused on homogeneous graphs. However, real-world graphs are typically heterogeneous in nature, consisting of multiple types of nodes and/or edges. For example, a citation graph represents heterogeneous information, involving authors, articles, as different node types. The edges model various types of relationships, e.g., one article citing the other, one author writing an article. To take full advantage of such heterogeneity, recent GNN models define exclusive parameters and data-paths for each of the types, i.e., relational GNNs (RGNNs).

RGNN poses three major challenges to the existing GPU compute stack due to its inherent computation patterns, the gap between the programming interface and the kernel APIs, and the high cost of kernel code optimization due to its coupling with data layout and heterogeneity. The first challenge with GNN implementations on GPUs stems from their need to traverse graphs and gather/scatter tensor data in order to use high-performance general matrix multiply (GEMM) kernels to implement message passing. During this step, graph structure and layout have major impact on the memory access patterns and execution throughput [29, 34]. (examples and details in Section 3). Furthermore, as the connectivity of the input graph is involved in the gather computation, the computation patterns of GNNs are affected not only by the model definition but also by the graph. Such data-dependent behavior precludes any one-size-fits-all optimization strategy when executing GNNs. Furthermore, RGNN introduces new complication to the design space due to the need for the operations to account for heterogeneity. We detail this in Section 2.

The second challenge in RGNN implementation is due to the lack of an abstraction layer between the programming interface and kernel APIs, which results in both suboptimal schedules and extra data movement. For example, the DGL

*Significant portion of the work is done during internship at Amazon Web Services (AWS).

HeteroConv operator uses a Python native loop to separately launch kernels for each of the edge types in a heterogeneous graph, leading to serial execution of small GPU kernels that underutilize GPU execution resources. PyG FastRGCNConv utilizes batched matrix multiplication `bmm()` when applying a typed linear layer to features of nodes to unleash parallelism. However, the weight matrices are redundantly copied along the batch size dimension in order to match the dimension of the input features. Pigeon avoids such unnecessary copying activities by having typed linear transforms operate on views of tensors, and decouples the materialization of its operands from the source-level expression (Section 3.1.3).

Third, high-performance neural network implementations have historically been based on pre-built libraries, e.g., cuBLAS [24]. GNNs make this less practical because the number of required kernels is amplified by the number of adjacency-matrix storage formats such as CSR and COO [19]. For example, cuSPARSE only supports Blocked-Ellpack in select APIs [23]. The typed edges and nodes of RGNN further exacerbate the problem, which makes the traditional pre-built libraries even less adequate and compels framework developers to either painstakingly develop optimized layers from scratch or settle for slow implementation. For example, it took more than a month for a full-time employee to implement and deploy the typed linear layer of RGNN in DGL [21].

To systematically address these challenges, we propose the Pigeon two-level intermediate representation (IR) and an associated code generator framework. This solution 1) represents the key properties of RGNN models to *bridge the gap* between the programming interface and available kernels, 2) *decouple* models, data layout and operator-specific schedule from each other to reduce programming efforts, and 3) *express and leverage* optimization opportunities in inter-operator transforms, data layout, and operator-specific schedules.

The top level, i.e., the inter-operator level, of the Pigeon IR supports expression of optimization among the operators, e.g., kernel fusion and selection of optimizations based on the graph characteristics and knowledge of the operator semantics. At the lower level, i.e., the intra-operator level, the IR design decouples the data access schemes, associated with the sparse data format and intermediate data layout, from the compute schedules. The two-level IR design also incorporates operator-specific schedule and optimization to the code generator. For example, the node-traversal and/or edge-traversal operator schedules involve graph-aware loop transforms such as loop unrolling that enables inter-iteration overlapping.

The contribution of this work is as follows.

1. We propose Pigeon two-level IR and code generation framework to allow systematic optimization and code generation for RGNN training and inference on GPUs. It *bridges the gap* between the programming interface and available kernels, *decouples* models, data layout and operator-specific schedule from each other, and *leverages* optimization opportunities from the three aspects.
2. We show that, by basing the Pigeon code generator on two generalized CUDA templates, i.e., a GEMM template and a node and/or edge traversal template, Pigeon achieves up to $7.8\times$ speed-up in inference and up to $5.6\times$ speed-up in training compared to the best among the state-of-the-art systems [9, 30, 31] when running RGCN, RGAT and HGT [2, 13, 26] on heterogeneous datasets provided by DGL and Open Graph Benchmark (OGB) packages [1, 4–6, 11, 27]. Pigeon also encountered fewer out-of-memory (OOM) errors, which is significantly alleviated by the optimization mentioned in Section 3. In fact, Pigeon incurs no OOM error for all the datasets tested in this paper.
3. We devised a compact tensor materialization scheme and a linear operator fusion pass as options. The best combination of options varies across models and/or datasets and further obtain up to $2.0\times$ speed-up in inference and $2.2\times$ speed-up in training compared with our basic generated code mentioned in Section 2.

The rest of this article is organized as follows. Section 2 introduces the background of RGNNs and demonstrates the performance challenges. Section 3 details the Pigeon design and implementation. Section 4 evaluates our work. Section 5 introduces the related work. Section 6 briefly summarizes our ongoing and future efforts. Section 7 concludes this article.

Artifacts will be released with the publication of this paper.

2 Background and Motivation

2.1 RGNN Formulation and Operators

GNNs are feedforward neural networks that propagate and transform layer-wise features. A widely-employed model is graph convolutional network (GCN) [16], which relies on the layer-wise message passing scheme. Formally, a GCN layer is defined as $h^{(l+1)} = \sigma\left(D^{-\frac{1}{2}}AD^{-\frac{1}{2}}h^{(l)}W^{(l)}\right)$, where $W^{(l)}$ denotes a trainable weight matrix of the l -th layer, σ is an activation function and $h^{(l)}$ is the l -th layer node representation. A is the adjacency matrix and D is a diagonal matrix of node degrees. We initialize h_v^0 with node input features.

RGNNs extend GNNs to relational graph data, i.e., heterogeneous graphs. For example, the relational graph convolutional network (RGCN) [26] extends GCN to aggregate messages from different relation types together. An RGCN layer is defined as $h_v^{(l+1)} = \sigma\left(\sum_{r \in R} \sum_{u \in \mathcal{N}_v^r} \frac{1}{c_{v,r}} W_r^{(l)} h_u^{(l)} + W_0^{(l)} h_v^{(l)}\right)$, where \mathcal{N}_v^r denotes the set of neighbors of node v in relation $r \in R$, $h_n^{(l)}$ is the l -th layer node representation of n . $W_r^{(l)}$ and $W_0^{(l)}$ are trainable weights of the l -th layer corresponding to relation r and to v itself, respectively. $c_{v,r}$ is a problem-specific normalization factor.

A typical element in more complicated RGNN models is attention. Figure 2 shows the layer of a relational graph

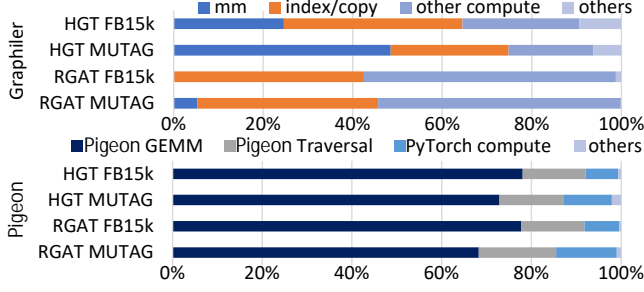


Figure 1: Breakdown of Graphiler (upper) and Pigeon (lower) running inference. mm stands for matrix multiply and includes sparse matrix-matrix multiplication.

attention network (RGAT) [2] and heterogeneous graph transformer (HGT) [13]. Edge attention is produced by operations among weights and features of the source and destination nodes. Both RGAT layers and HGT layers apply to edge attention the edge softmax operator, $\sigma_{sm}(\cdot) = \exp(\cdot) / \sum \exp(\cdot)$, which normalizes the attention of all incoming edges. Typed linear layer $W_{\tau(n)}$ is a linear transform whose weights are dependent on the type of input node $\tau(n)$. It is a scalar that emphasizes the message associated with the same edge during the subsequent node aggregation stage.

2.2 Implementing Typed Linear Layers

There are two ways to implement the typed linear transform in existing systems, i.e., batched matrix multiplication (BMM) `bmm()` and segment matrix multiplication (segment MM).

Sorting nodes by the node type transforms the node features tensor into segments of node features of the same node type. When applying a typed linear layer to node features, one can simultaneously apply the corresponding weight tensor of the node type to each segment. This is segment MM.

Using BMM is applicable even when the nodes are not presorted. `bmm()` treats its two operands as two batches of matrices and performs matrix multiplication for each pair. This causes redundant weight replication.

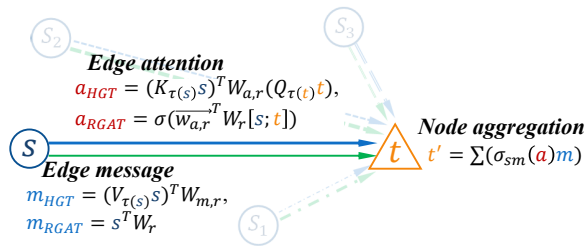


Figure 2: A typical RGNN layer for node classification. n and n' are node features. For edge attention and message, we show both the formula of HGT and RGAT. Weights W_{\cdot} , \vec{w}_{\cdot} differ by relation type r . Weights $W_{\tau(n)}$ differ by the node type $\tau(n)$ of n . σ is leaky rectified linear unit (ReLU) in the case of RGAT. σ_{sm} stands for edge softmax. $[s; t]$ concatenates s, t .

Table 1: Count of FLOPs involved in calculating a_{HGT} shown in Figure 2. m, k, n stands for the number of heads, the input feature dimension, and the output feature dimension. $|V|$, $|E|$ and $|T(E)|$ are the number of nodes, number of edges, and number of edge types, respectively.

	Compute	Memory	# Launches
Linear layer	$2mkn$	$\frac{2mkn}{\text{TILE_WIDTH}}$	$\min(V T(E) , E)$
Inner product	mn	$2mn$	$ E $

2.3 RGNN Performance Characteristics

RGNNs incur high portion of memory-intensive operations [29, 34]. Furthermore, unlike fixed neurons connectivity in non-graph neural networks, the performance of RGNN is strongly affected by both the model and the graph dataset.

GPUs are excellent at matrix multiplication whose high computation complexity can leverage the massively parallel compute units provided by GPUs, and the input data could be sufficiently reused to allow the memory bandwidth to keep up with the computation throughput. The performance can drop significantly in situations with fewer data reuse opportunities.

In non-graph neural networks, most linear transforms, e.g., convolutional layers, can be efficiently implemented as GEMM kernels. GEMM takes up most of the execution time due to its cubic complexity.

In contrast, RGNNs spend a much larger portion of their execution time on non-GEMM, memory-intensive operations. Furthermore, memory intensiveness is dynamic depending on factors such as average degrees and number of relations in the graph. Take calculating a_{HGT} in Figure 2 as an example: Multiplying $W_{a,r}$ with $(Q_{\tau(t)t})$ and then multiplying the product with $(K_{\tau(s)s})$ can be done with a typed linear layer, followed by an edge-wise vector inner product. Since the result of the linear layer transform is the same for each (source node, edge type), to save computing, the system can instead calculate the result for each (source node, edge type) instead of calculating it for each edge. In the mag dataset, this will save more than 70% of the launches. When this happens, the ratio of launches between the two types of layers further amplify the memory-intensiveness. This procedure is outlined in Table 1.

To better illustrate the points, Figure 1 breaks down HGT and RGAT inference on FB15k and MUTAG. Section 4.1 details the system configurations and datasets. This experiment measured Graphiler [31], which executed compiled TorchScript code and delivered the best inference performance among existing systems tested in this work. Figure 1 shows that indexing and copy takes up significant portion, and the portion of GEMM operations varied with the graph. By comparison, Pigeon achieves performance improvements by lowering the logic to GEMM as much as possible and assembling kernels with flexible access scheme to gather and scatter data on the fly to eliminate copy or indexing procedures.

Table 2: Features of Pigeon and previous GNN end-to-end compilers [9, 30, 31]. “Operator” is abbreviated as “OP”.

Name	Optimization target		Memory efficiency	Design space		
	Inference	Training		Data layout	Intra-OP schedule	Inter-OP optimization
Graphiler	✓		✓			✓
Seastar	✓	✓				✓
HGL		✓	✓			✓
Pigeon	better	better	better	✓	✓	✓

2.4 Motivation of This Work

To address the performance challenges in RGNN systems due to both RGNN inherent computation pattern and the system design, we propose Pigeon IR and code generation framework. Through the IR design that *decouples* and *expresses* the model semantic, data layout and operator-specific schedules, Pigeon allows the use of these opportunities and the integration of all three aspects into the design space. Table 2 shows the feature comparison of Pigeon with existing systems.

3 Design and Implementation

This section details the design and implementation of the Pigeon IR-based code generator and runtime.

3.1 Overview

3.1.1 Workflow and System Components

The Pigeon system consists of the programming interface to specify the input, the code generator and Python runtime modules. The code generator takes in the model definition and generates both CUDA kernels and host functions that configure and invoke the CUDA kernels.

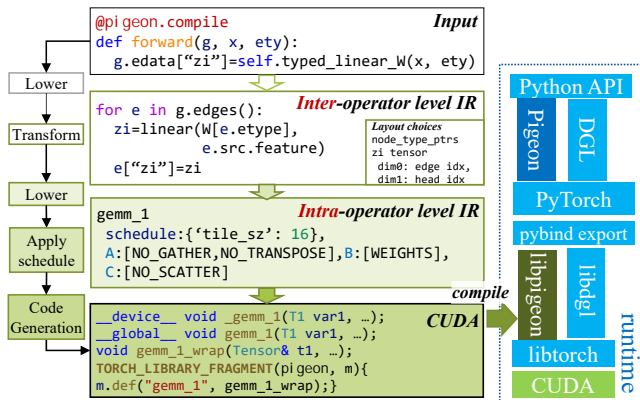


Figure 3: Pigeon workflow and software architecture.

Figure 3 uses an example to illustrate the workflow. The input is an excerpt of DGL code invoking a typed linear layer on input node features. Applying the decorator `@pigeon.compile` triggers a transpiling pass to lower the

code into Pigeon inter-operator level IR. In this example, the typed linear transform `typed_linear_x` can be efficiently implemented as GEMM kernels. To this end, Pigeon lowers the transform to an operator instance derived from the GEMM template at the inter-operator level. After the analysis and optimizations at the inter-operator level, Pigeon further lowers the code to a detailed GEMM specification at the intra-operator level. The intra-operator level IR indicates that the GEMM operation should use the default tile width of 16 and be performed without scatter, gather or transpose applied to the input or output matrices. Eventually, Pigeon generates a segment MM kernel `gemm_1`, which is detailed in Section 2.2.

The generated code is compiled into a shared library where the host functions are exported through the `pybind11` utilities. Pigeon falls back to existing routines in PyTorch when certain operators are not yet supported. During runtime, the precompiled functions are loaded and registered as subclasses of PyTorch `autograd.Function`.

3.1.2 Pigeon Two-Level IR

Central to the code generator is the two-level IR: the inter-operator level IR defines the model semantics as sets of operators, and provides the facility to express layout choices; the intra-operator level IR provides the facility to express templates specialization and lower them to CUDA kernels. The two-level design decouples the inter-operator transforms from operator-specific schedules, and captures optimization opportunities from both perspectives.

Model definitions in the Pigeon inter-operator level IR abstract away the data layout and only expresses the model semantics. The way in which the data per node and the data per edge are materialized into PyTorch Tensors and how adjacency is encoded are decoupled and undetermined at this point. Lowering to the intra-operator level IR will not happen until the data layout and sparse adjacency are determined. The intra-operator level IR is currently based on two CUDA kernel templates, the GEMM template, and the node and/or edge traversal template. IR at this level instructs how templates should be specialized to generate the CUDA code.

The Pigeon two-level IR enables concerted but decoupled choices of intermediate data layout and compute schedules: For example, in Figure 3, the semantics of the model is decoupled from the layout choices. During lowering, Pigeon encodes the information of the model semantics and layout

choices in intra-operator level IR with specific access scheme.

Listing 1: Expressing the attention calculation in a single-headed RGAT model using Pigeon inter-operator level IR.

```

1  def edge_softmax(g):
2      for e in g.edges():
3          e["attn"] = exp(e["attn"])
4      for n in g.dst_nodes():
5          n["attn_sum"] = 0.0
6          for e in n.incoming_edges():
7              n["attn_sum"] += e["attn"]
8      for e in g.edges():
9          e["attn"] /= e.dst["attn_sum"]
10
11  for e in g.edges():
12      zi=e.src.feature * W[e.etype]
13      zj=e.dst.feature * W[e.etype]
14      e["attn"] = leakyrelu(inner_prod(
15          attn_vec[e.etype], concat([zi,zj])))
16  edge_softmax(g)

```

Table 3: Pigeon inter-operator level IR constructs.

Graph variable and methods			
graph variable	g	edge iterator	g.edges()
node iterator	g.dst_nodes(), g.src_nodes()		
neighbor iterator	n.incoming_edges(), n.outgoing_edges()		
weight slicing, e.g.,	W[e.etype]		
Attributes			
nodes	e.src, e.dst	types	e.etype, n.etype
input data, e.g.,	n.feature	produced data, e.g.,	e["attn"]
Operators			
GEMM-eligible computation, e.g.,	linear(), outer_prod()		
GEMM-ineligible computation, e.g.,	inner_prod()		
Manipulation, e.g.,	reshape(), concat()		

3.1.3 Tensor Materialization and Compaction

The Pigeon inter-operator level IR deliberately abstracts away the data layout from the model semantics. As exemplified by Listing 1, the IR only expresses the association of variables with nodes or edges, e.g., `e["attn"]` and `n["attn_sum"]`, without dictating the mapping of elements in the conceptual variable to the memory space. This opens up high-level optimizations, e.g., compaction, and architecture-specific optimization, e.g., padding the innermost dimension.

In this work, we devised a technique compact materialization, that is enabled by the decoupling between model semantics and data layout. Notice that certain edge data are merely determined by source node features and edge types, e.g. m_{HGT} in Figure 2. Rather than computing and storing such data for each edge, we instead compute and store the data once for each (edge type, unique node index) pair, reducing the resources spent on computing and storing common subexpressions. As exemplified in Figure 4, the materialized tensor involves 8 rows if each row vector corresponds to z_i of an edge. Alternatively, the system can materialize a tensor

with only 5 rows where each row vector corresponds to z_i of an (edge type, unique node index) pair. We call the former vanilla materialization and the later compact materialization.

Pigeon readily supports alternative materialization schemes as it decouples the layout/access scheme, i.e., logic to determine the row number to locate the vector in the tensor, from compute schedule. For the vanilla scheme, the row number is the edge index specified by the sparse adjacency. For the compact scheme, it is a unique nonnegative integer assigned to each (edge type, unique node index). We precompute this mapping and store it in a CSR-like format.

3.1.4 Programming Interface

In order to program the model as input to Pigeon system, one can use the Pigeon inter-operator level IR itself. To reuse code, one may define a function using Pigeon inter-operator level IR and invoke it during programming. Lines 1-9 in Listing 1 show an example. The input can then invoke this function whenever normalization by sum is needed.

Pigeon provides a Python decorator, `@pigeon.compile`, to take existing PyG or DGL forward propagation logic and generate code for it, as exemplified by the input in Figure 3. The decorator, when applied to a method, invokes a simple transpiling pass that replaces the PyG and DGL method calls, e.g., SpMM/SDDMM, with Pigeon’s implementation in the inter-operator level IR, and replaces supported constructs from PyG and DGL, e.g., `g.canonical_etypes()` loop, with expressions in Pigeon IR.

Pigeon can generate code for backward propagation with only forward propagation inputted, as Section 3.5 will discuss.

3.2 Pigeon Inter-Operator Level IR

The inter-operator level IR is designed to decouple operator semantics from data layout and access schemes. It follows the Python grammar but involves a few new constructs. Listing 1 illustrates how the attention calculation in a single-headed RGAT layer could be expressed using Pigeon inter-operator level IR. As shown in Listing 1, the message generation and aggregation stages are expressed as foreach edge loops starting from line 2, line 8 and line 11, and foreach node loop starting from line 4. To accumulate data from the incoming edges, the `n.incoming_edges()` iterator is used. Noteworthy, the data layout, i.e., how to access the input and output data per edge or per node, and how to figure out the incoming edges associated with each node, are abstracted away in Listing 1. Table 3 lists the Pigeon IR features at this level.

3.2.1 Data Layout Specifications

Decoupled from the model semantics, the other element in Pigeon inter-operator level IR is the data layout specifications. It defines 1) how the conceptual data associated with each node or edge are materialized as PyTorch tensors, i.e., the

materialization discussed in Section 3.1.3, and 2) the sparse adjacency encoding needed during execution. At the inter-operator level, data layout specifications are decoupled from the model semantics and not influencing the transform passes in this level. However, they determine the data access scheme and make a difference when generating CUDA code at the intra-operator level. Pigeon inter-operator level IR bookkeeps the specifications and they are passed to the intra-operator level during lowering. The intra-operator level operator instances choose the data access scheme corresponding to the data layout specifications during assembling the kernel code.

3.3 Pigeon Intra-Operator Level IR

The Pigeon intra-operator level IR serves between the inter-operator level IR, and the generated CUDA code. At this level, the IR should encode specifications to emit CUDA code, and provide sufficient information specific to each operator invocation to the transform and lowering passes at the inter-operator level. These tasks are mainly carried out by the basic elements in IR at this level, lower IR operator instances. They provide the methods to generate specialized CUDA code for the operators, to apply operator-specific schedule, and to return necessary information on operator selection and kernel fusion feasibility to the passes at the inter-operator level.

Pigeon’s code generator ultimately lowers the IR to two basic constructs, the GEMM template, and the traversal template. Algorithms 2 and 1 illustrate the edge traversal template and the GEMM template. The node traversal template is similar to Algorithm 2, and we will revisit it in Section 3.3.3. For simplicity, closures are routines specialized for the specific instances derived from the two templates and involve 1) function arguments, e.g., number of rows, etc, 2) special registers, e.g., `threadIdx`, and 3) loop variables.

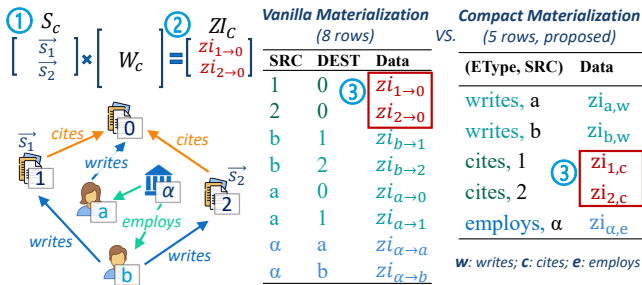


Figure 4: Calculating z_i in Figure 3 on a citation graph. This procedure ① gathers the features of the source nodes into a matrix, ② performs the GEMM computation and ③ scatters the output features to rows in the output tensor (vanilla vs. compact materialization). All data are in the device memory.

Algorithm 1: Pigeon’s GEMM template in pseudo-code. Each instance is assigned a unique identifier `kid` and gets specialized closures **FuncName**<`kid`>.

Input: References of Tensor A, B, C , adjacency, etc.

```

1 tileRowRange, tileColRange ← GetRange<kid>();
2 foreach idxTileRow ∈ tileRowRange do
3   foreach idxTileCol ∈ tileColRange do
4     LoadAToShmemIfInRange<kid>();
5     LoadBToShmemIfInRange<kid>();
6     __syncthreads();
7     C_reg ← A_shmem × B_shmem;
8     __syncthreads();
9   StoreCIfInRange<kid>();

```

3.3.1 The GEMM Template

As shown in Algorithm 1, the GEMM template is based on squared tiled matrix multiplication. The GEMM template starts with working out the work assignment per block during the `GetRange`<`kid`> enclosure. The `idxTileRow` and `idxTileCol` whose range is determined by `GetRange`<`kid`> is used to position the workload. Typically, it is the coordinate of the tile of the output matrix. Factors that affect loading schemes `LoadAToShmemIfInRange`<`kid`> and `LoadBToShmemIfInRange`<`kid`> involve whether gather lists or transpose needs to be applied on the fly. A gather list is needed when the kernel needs to locate the row by mapping from one or two from edge index, node index, edge type, and compact row number to another. This is determined by the slicing elements of the weights, enclosing loop, and materialization option in the inter-operator level. The required information will be passed during the lowering. The operator instance then accordingly chooses the data access scheme code piece for kernel code generation. The storing scheme `StoreCIfInRange`<`kid`> depends similarly on whether a scatter list will be applied. Atomic intrinsics are used in the case of multiple simultaneous updaters.

3.3.2 The Traversal Template

In Algorithm 2, the edge type, node indices retrieval scheme in line 5 – line 7 depend on the sparse adjacency encoding. Similarly to the GEMM template, when a row vector needs to be loaded or stored, the tensor materialization scheme determines how the row is located in the materialized tensor. All statements are initially inserted into the innermost loop.

When Pigeon finishes the loop transforms, it signals the operator instance derived from the traversal template to define work assignment on line 1 in Algorithm 2. We use a simple hard-coded scheme. For example, if the loop nest is three levels, as exemplified by Algorithm 2, we assign the outermost loop, i.e., `idxEdge` or `idxNode` loop, to each block.

Algorithm 2: Pigeon’s edge traversal template in pseudo-code. Similarly to Algorithm 1, each instance gets specialized **FuncName<kid>**.

Input: References of input and output tensors. Other necessary data, e.g., adjacency.

```

1 eRange, hRange, fRange ← GetRange<kid>();
2 foreach idxEdge ∈ eRange do
3   foreach idxHead ∈ hRange do
4     foreach idxFeat ∈ fRange do
5       eType ← GetEType<kid>();
6       srcIdx ← GetSrcId<kid>();
7       dstIdx ← GetDstId<kid>();
           // initial insertion point

```

3.3.3 Operator-Specific Schedule

Each instance derived from the GEMM template provides the options to apply a coarsening factor in $\{2, 4\}$, to choose the tile width in $\{16, 32\}$, and to apply `__launch_bounds__` that limits the number of registers in exchange for more active warps. Coarsen factor is the number of elements that each thread deals with in each of the loading, computing, and storing stages. When applied, each block still works on the same assignment, but its number of threads shrinks by the factor [19]. We also allow a per-row scalar to be applied to A tiles. This eliminates the extra memory-intensive traversal to perform weighed summation of vectors by attention or norm.

As for the traversal template, we enable graph-semantic-aware loop transform: a `foreach` loop over the edges is equivalent to a `foreach` loop nest iterating all the incoming/outgoing edges of each destination or source nodes. Enhancing the generic loop transform with this specific rule allows Pigeon to take advantage of graph semantics to open up the trade-off between more data reuse opportunities and greater parallelism. As mentioned in Section 3.3.2, in each instance derived from the traversal template, initially all statements are placed in the innermost loop. To optimize, loop hoisting is invoked. In addition, the operator also provides a method, by default applied during lowering, to reduce global memory traffic by accumulating results within a thread and within a warp before atomically adding them to the data in global memory.

3.3.4 Operator Selection and Fusion

Transform and lowering passes in the inter-operator level need to get information about operator instances, specifically operator precedence and the feasibility of kernel fusion. Precedence is the mechanism Pigeon used to select the operator instance when there are multiple candidates. For example, an operator derived from the GEMM template can also be implemented by the traversal template, but this leads to lower performance due to not reusing data as much. To achieve good performance, by default, operators derived from the GEMM template are

assigned a higher precedence than those derived from the traversal template unless otherwise specified. Instances that fall back to PyTorch have the lowest precedence.

Operator instances also provide methods that determine the feasible operators to be fused with in the IR, and that return the new fused operator. Operator instances derived from the GEMM templates can be fused with the output user if the user multiplies the row vectors in the GEMM output with scalars and if the two operators are in the same loop (nest). Operator instances derived from the traversal template can be fused with each other as long as they are in the same loop (nest). If the pass in the inter-operator level determines some variables are created and merely used inside the fused operator, it passes that knowledge to the method so that the variable no longer needs to be created in the global memory.

3.3.5 Sparse Adjacency Encoding

At the intra-operator level, the templates work for any sparse adjacency encoding as long as specific interfaces are implemented. For example, the edge traversal shown in Algorithm 2 works as long as the closures `GetEType<kid>`, `GetSrcId<kid>` and `GetDstId<kid>` are implemented: If the sparse adjacency is COO, `GetSrcId<kid>` is a subscript operator applied to the row indices array. If it is CSR, then `GetSrcId<kid>` is a binary search into the row pointer array.

3.4 Transform and Optimization

3.4.1 Linear-Operator Fusion

We propose linear operator fusion as one of the inter-operator level optimization. When a linear operator, e.g., linear layer, and inner product, is followed by another linear operator, their order may be switched. For example, for a_{RGAT} as shown in Figure 2, we may calculate $\vec{w}_{a,r}^T W_r$ first instead. Such an order change may reduce the strength in some cases. We implement the pass to switch the orders of linear operators whenever this produces an operator between weights. To determine eligibility, the operator instances provides a method returning if itself is a linear operator. For simplicity, rewritten operator instances use PyTorch `bmm()` to compute the product of weights and apply PyTorch built-in slicing if necessary.

3.4.2 Graph-Semantic-Aware Loop Transform

Similarly to the discussion in Section 3.3.3, loop transform at this level is also augmented with the graph-semantic-specific equivalence rule. Loop transform is applied during the lowering pass to canonicalize and fuse loops in order to more thoroughly identify kernel fusion opportunities.

3.4.3 Lowering Inter-Operator Level IR

To lower the IR to the intra-operator level, Pigeon greedily lowers every eligible operator to instances derived from

GEMM templates. Then, it fuses each remaining regions and lower them to as few traversal instances as possible.

To achieve this, Pigeon scans the code three times. Each time, it checks if the current operator can be lowered to an instance of a specific precedence. The first time, it attempts GEMM-template-derived instances. In the next scan, it attempts the traversal-template-derived instances. All the remaining operators will be lowered to PyTorch function calls in the third scan. Whenever an operator can be lowered, Pigeon invokes its method to mark all subsequent operators that can be fused and skip them in this scan. After this scan, the operators are lowered and fused. Before the second scan, it canonicalizes the for loops and fuse loop nests whenever possible to discover kernel fusion opportunities.

3.5 Backward Propagation

Similarly to PyTorch, Pigeon supports auto differentiation by maintaining a look-up table that maps operators to their backward propagation counterparts. Pigeon first emits the backward propagation via inter-operator level IR, and keeps the required gradients while removing unused gradients and logic to compute them. The lowering and code generation schemes are similar to those in forward propagation. The difference is that the backward propagation follows the kernel boundary established during the lowering of the forward propagation, so that the generated host functions pair with each other. To achieve this, Pigeon assigns metadata to each operator in forward propagation and bookkeeps whenever operator fusion occurs during lowering. Pigeon will try its best to fuse the corresponding operators as well during lowering backward propagation. If it fails, it will fuse the host functions of the corresponding operators during code generation.

3.6 Code Generation

The code generation procedure emits code based on the CUDA kernel specifications detailed in the form of intra-operator IR. Kernel code generation is fairly straightforward and is implemented using a template-based approach.

Kernels are emitted as `__device__` functions. Pigeon then wraps them into `__global__` functions, where the arguments are deduplicated to meet the restrict pointer qualification. If applicable, Pigeon emits the `__launch_bounds__` directive. Pigeon then emits the host functions that configure grids and blocks, gets raw pointers from the `libtorch.at::Tensor` references, and launches the corresponding kernel. Host functions are exported through the `pybind11` utilities.

A pass scans all the procedures to collect a list of pre-processing required for the input dataset, i.e., transposition, converting COO to CSR, etc. The code generator emits the invocation necessary before training/inference.

3.7 Discussion on Design Choices

3.7.1 Extensibility

Pigeon is designed as an extensible framework to prototype new techniques and evaluate them for our long-term code optimization research for RGNN. First, inter-operator optimization can be prototyped as inter-operator level passes. Second, the new sparse adjacency encoding and intermediate data layout can be supported by adding the corresponding intermediate data and adjacency access scheme discussed in Section 3.2. Third, kernel optimization can be prototyped as a kernel template and operator instances based on it. Alternatively, it can be implemented as operator-specific schedules. We will briefly discuss our next steps in Section 6.

3.7.2 Avoid Weights Replication

Some systems replicate weights during forward propagation. For example, one way to enable edge-wise computation to access a typed weight tensor is to make a copy of the weight slice for each edge corresponding to its relationship type. The reason may be two-fold. First, this serves as a means to leverage PyTorch’s expressive APIs, such as batched matrix multiplication `bmm()`. Second, replication might help to achieve greater parallelism.

However, this adds extra data movement to both forward and backward propagation. Pigeon instead keeps a single copy of the weights, but adapts the access schemes in each generated kernels to it. As Section 4 shows, our system still achieves competitive performance and higher memory efficiency.

4 Evaluation and Discussion

We evaluate Pigeon with the following questions to answer.

1. How does the performance of Pigeon compare with state-of-the-art systems? How does Pigeon achieve it?
2. How much improvement do the two proposed techniques detailed in Sections 3.1.3 and 3.4.1, i.e., compaction materialization and linear operator fusion, make?

Sections 4.2 and 4.3 answers Question 1–2, and Section 4.4 further analyzes the performance implication of the two proposed techniques through case study.

4.1 Methodology

To assess performance, we measure the inference and training time of Pigeon system and others on a single-GPU computer. Its main hardware components involve one Intel Core i9-9900K CPU, 128 GB dual channel memory, and one Nvidia RTX 3090 GPU with 24GB memory. The operating system

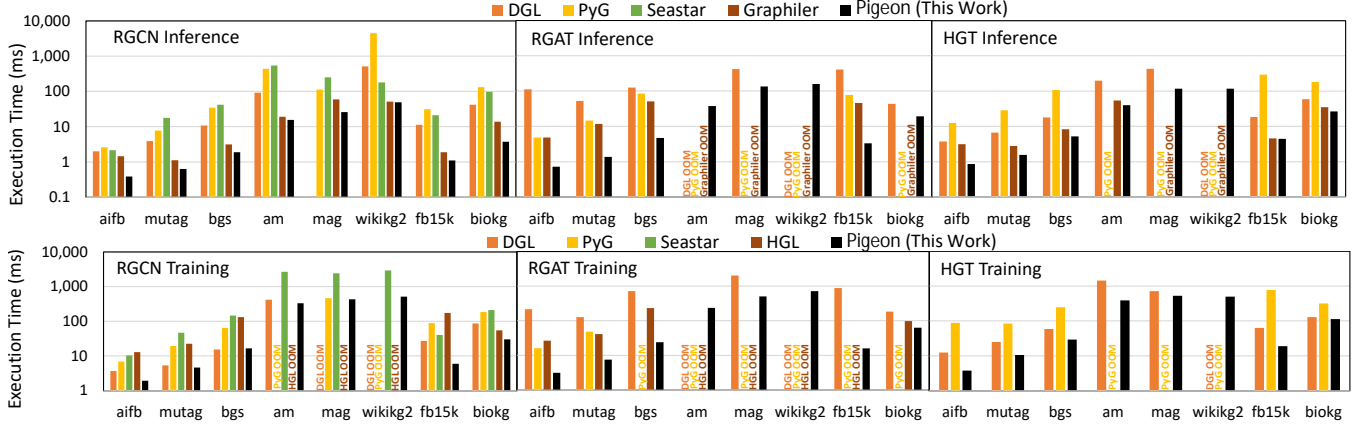


Figure 5: Comparing the performance of Pigeon best optimized code with previous work. Table 4 shows the datasets used.

is Ubuntu 18.04.5, with kernel version 5.4.0-135. The CUDA and driver version are 11.6 and 510.108.03, respectively.

We have not fully implemented the code generator due to limited manpower. Manual coding following the design and procedures in Section 3 is used. The code produced involves more than 3K C++ kernel code, 5K C++ code to define host functions, 2K Python code to define subclasses of Pytorch `autograd.Function`, and 2K Python code that provides common utilities. These measures exclude comments.

As shown in Table 4, we use public datasets prepared by DGL [28] and OGB [11]. We measure (1) inference and (2) training time on three RGCN models, i.e., RGCN [26], RGAT [2], and HGT [13], with previous work, i.e., DGL [28], PyG [7], Seastar [30], Graphiler [31], and HGL [9]. We ported Seastar artifacts to the same version of CUDA and Python packages as Pigeon depends on because one of Seastar’s dependency, `dgl 0.4`, used an API deprecated since CUDA 11.

To best align with the hyper-parameters prior work used in their evaluation, we set the input and output feature dimension as 64, and number of heads as 1. We measure the inference and training time of the single layer used. In training, in order to obtain a loss, we compute the negative log likelihood loss by comparing the output with a precomputed random label tensor. For each case, we run the full graph inference and training for at least 10 epochs and average the elapsed time. To align with the existing system, nodes are presorted to enable segment MM for typed linear layers.

4.2 Comparison with Prior Work

For performance of DGL and PyG, we measure all public implementation of these models from DGL, PyG, and Graphiler artifacts. PyG provides two RGCN convolution layers: `RGCNConv` places nodes in segments of the same type but launches separate kernels for each of the node types, leading to device underutilization. `FastRGCNConv` replicates weights and uses `bmm()`. It is consistently faster than the `RGCNConv`

Table 4: Heterogeneous graph datasets [1, 4–6, 11, 27] used in our evaluation. The numbers reflect the default preprocessing by the OGB and DGL packages, e.g., adding inverse edges.

	# node types	# edge types	# nodes	# edges	density ($\times 10^{-6}$)
aifb	7	104	7.262K	48.81K	925.5
mutag	5	50	27.16K	148.1K	200.7
bgs	27	122	94.81K	672.9K	74.86
am	7	108	1.885M	5.669M	1.595
mag	4	4	1.940M	21.11M	5.611
wikikg2	1	535	2.501M	16.11M	2.576
fb15k	1	474	14.54K	620.2K	2933
biokg	5	51	93.77K	4.763M	541.6

implementation. Similarly, DGL’s built-in segmentMM-based RGCN layer is faster than other DGL implementations. For HGT, the DGL segmentMM-based `HGTConv` primitive generally has the best performance. In the cases where some variants encounter OOM errors, we choose the best among those that run without issues. Some cases are missing due to insufficient operator support, such as HGL on HGT and Graphiler on training. We do not measure HGL in inference because it is designed for optimizing training.

Figure 5 shows that the best optimized Pigeon code consistently outperforms state-of-the-art systems in all cases, except for the case of RGCN training on bgs, where our speed-up is 93% of DGL. We achieve speed-up of up to $14\times$ in inference and speed-up of up to $6.4\times$ in training against the best among state-of-the-art systems. On geometric average, Pigeon gets $1.94\times$, $7.7\times$, $1.63\times$ speed-up in inference via RGCN, RGAT, and HGT, and $1.80\times$, $5.1\times$, $2.4\times$ speed-up in training RGCN, RGAT, and HGT, respectively.

There are two reasons why Pigeon is more efficient in device memory usage. First, Pigeon only keeps a single copy of weights, as discussed in Section 3.7.2. Replicating weights also affects backward propagation because the gradient of each individual weight will be derived, occupying extra mem-

ory. Second, our compact materialization reduces memory and redundant computation, and we cover this in Section 4.3.

We see close performance achieved by Graphiler in RGCN and HGT inference. Graphiler leverages PyTorch utilities to convert the Python code to TorchScript and compile it before execution and utilizes edgewise parallelism for edgewise computation. Similarly to RGCNConv, it places node features into segments of the same type, but runs separate kernels to perform a typed linear transform. DGL and PyG under similar configurations achieve competitive performance. However, when it comes to RGAT, Graphiler suffers from performance degradation. Because Graphiler relies on pre-programmed fused kernels to deliver a significant portion of the performance boost [31], we postulate that the degradation is due to the non-exhaustiveness of these pre-programmed kernels [32]. This suggests the drawbacks of compiler design without a code generation mechanism. Besides, it can be challenging to generalize Graphiler’s approach to training because of the limited TorchScript auto-differentiation support. For example, dict object construction is not supported, but it is a common way to express data associated with nodes and edges.

Noteworthy, even without compaction and linear-operator fusion, Pigeon still outperforms existing systems with only 4 slowdown cases, as Table 6 shows. Additionally, the unoptimized Pigeon code triggers fewer OOMs than existing systems, with the only exception where the RGAT inference is run on mag. As the breakdown in Figure 1 shows, the cause of the performance improvement is the 1) eliminating redundant data movement by instead assembling kernels with flexible access scheme to gather and scatter data on the fly, and 2) lower kernels to GEMM as much as possible.

4.3 Effects of the Two Proposed Techniques

Now, we study the effects of compact materialization and linear-operator fusion. The two techniques are detailed in Sections 3.1.3 and 3.4.1. We investigate their effects on the two more complicated models, RGAT and HGT.

Table 5 shows the speed-up on top of Pigeon unoptimized code by these two optimizations. Due to compact materialization, when running RGAT on mag and wikikg2, Pigeon no longer triggers OOM errors. In addition, in some cases, the layout speeds up the execution as well due to the common subexpression elimination brought forth by the layout. Compact materialization is hardly possible without a code generation scheme or an IR design that decouples the model semantics, data layout, and operator-specific schedule.

Furthermore, Table 5 also shows that in terms of the two optimizations, the best configurations vary by model, input graph, and whether the task is training or inference. In particular, when training or inferring on RGAT, if the system chooses the best configuration for every input graph, on average the speed-up against unoptimized Pigeon code is $1.34\times$ in training and $1.49\times$ in inference. By comparison, the speed-up

Table 5: Speed-up on top of Pigeon unoptimized code due to compaction (C) and linear-operator fusion (F). The highest speed-up in each task is shown in bold ink.

		Training			Inference		
		C	F	C+F	C	F	C+F
RGAT	aifb	0.84	1.17	0.85	1.04	1.24	1.12
	mutag	0.76	1.14	0.80	1.16	1.25	1.33
	bgs	0.94	1.20	1.06	1.17	1.38	1.41
	am	0.85	1.15	0.93	0.94	1.34	1.08
	mag*	1*	OOM	1.02	1*	OOM	1.02
	wikikg2*	1*	OOM	1.08	1*	OOM	1.03
	fb15k	1.29	1.25	1.40	1.58	1.40	1.79
	biokg	2.16	1.26	2.20	1.93	1.41	1.97
Average		1.06	1.19	1.13	1.26	1.33	1.41
HGT	aifb	1.88	1.26	1.86	1.80	1.82	1.61
	mutag	1.28	1.16	1.32	1.46	1.54	1.36
	bgs	1.20	1.13	1.19	1.27	1.26	1.07
	am	1.11	1.10	1.07	1.29	1.30	0.93
	mag	1.08	1.08	1.14	1.11	1.11	0.90
	wikikg2	1.10	1.09	1.20	1.13	1.13	0.99
	fb15k	1.24	1.14	1.31	1.29	1.29	1.20
	biokg	1.04	1.02	1.15	1.05	1.05	0.95
Average		1.22	1.12	1.26	1.28	1.29	1.11

*Normalized by the performance with compact materialization (C) because the unoptimized version does not fit into GPU memory (i.e., OOM). These two rows are not counted when calculating the average.

against unoptimized Pigeon code fixed optimization could deliver on RGAT is $1.13\times$ in training and $1.41\times$ in inference.

4.4 Performance Analysis

To better understand the optimization Pigeon brings, we further study two cases, as shown in Figure 6. The compaction ratio of AM and FB15k, i.e., size of the materialized tensor against the vanilla materialization, are 57% and 26%, respectively. When running AM, the time GEMM instances take is significantly reduced, but the traversal instances, due to more complicated access scheme, take much longer time and offsets the improvements. By comparison, compaction brings performance improvement in FB15k. In both cases, linear operator fusion brings performance benefits due to significant reduction in GEMM time.

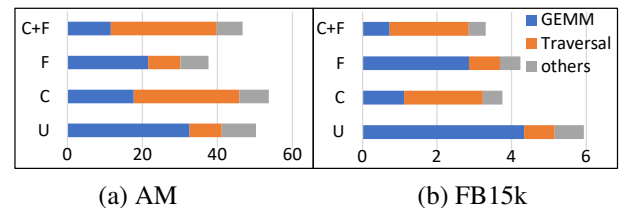


Figure 6: Breakdown of Pigeon RGAT inference on two datasets. The horizontal axes stand for duration in milliseconds. Cases with optimization, i.e., compaction (C) and/or linear operator fusion (F), and without (U) are presented.

Table 6: Speed-up of Pigeon unoptimized code vs. the best in state-of-the-art systems. Worst (W), average (M), and best (B) cases, and numbers of slowdown cases (#D) are shown.

	#D	Training			#D	Inference		
		W	M	B		W	M	B
RGCN	<u>1</u>	.93	1.64	3.8	<u>1</u>	.97	1.44	3.7
RGAT	<u>0</u>	4.4	4.93	5.6	<u>0</u>	5.3	6.39	7.8
HGT	<u>1</u>	.98	1.88	3.3	<u>1</u>	.77	1.19	2.0

5 Related Work

General GPU-accelerated GNN libraries. DGL [28] and PyG [7] are among the most popular GNN Python packages that allow easy development and evaluation of GNN models. DGL [28] proposes to implement GNN as SpMM/SDDMM operations. PyG’s key scheme is scatter and gather operations that switch between edge-parallel regions and node-parallel regions. Pigeon instead built upon GEMM and traversal templates. By lowering operators to GEMM as much as possible, Pigeon obtains better performance for RGNNs.

GNN end-to-end compilers. Seastar [30] proposes a vertex-centric compiler stack to generate performant kernels throughout the training and/or inference of the model. Graphiler [31] proposes to program the message passing data flow graph and devises several TorchScript transforms to emit highly optimized inference implementation. Similarly, HGL [9] is an RGNN compiler. These prior arts expose PyTorch tensors as operands of all operations to users, and replicate weight to unleash parallelism due to lack of support of flexible data access scheme and/or code generation. Thus, they more or less suffer from memory inefficiency and performance degradation.

Kernel code optimization. FeatGraph [12] proposes code optimization framework on top of TVM [3] for user-defined-function-enabled SpMM and SDDMM. Some work proposed optimization for specific GNNs kernels. GE-SpMM [14, 15], and work [10] propose optimized schedule for SpMM. Others involve Seastar [30], PyTorch-Direct [20], and TLPGNN [8]. As our work shows, SpMM/SDDMM is not the only essential kernel in end-to-end RGNN execution. And our work is orthogonal to these prior arts as they can be incorporated into Pigeon as operator-specific schedules or new templates.

Code generation. SparseTIR [33] and TACO [17] propose IR and code generator for sparse tensor operations. MLIR [18] proposes multi-level IR design for deep learning. Aligned with this direction, FusedMM [25] unifies the SpMM and SDDMM CPU kernel. They focus on single kernel code generation while we target the whole inference and training process. These works also are not designed specifically for RGNNs where edge types are involved in kernel schedule and adjacency encoding. While we do not intend to reinvent general-purpose sparse tensor code generator for completeness or performance, some of these works inspire us and may be incorporated to enhance the Pigeon code generator.

6 Future Work

Devise algorithms to select the layout, optimization and schedules according to model, input graph, and GPU architecture. One of the most important compiler research problems is the algorithm that makes choices among the candidates in the design space. Apart from the input graph, the specific microarchitecture of each GPU model also makes a difference due to the architecture-specific features available, e.g., asynchronous loading to shared memory since Ampere [22], and different microarchitecture characteristics in each model. Therefore, it is meaningful to investigate their impact and incorporate them into decision making.

Optimize data movement in minibatch training. Graphs cannot fit into GPU memory have to stay in host memory during RGNN execution. In each step, subgraphs are sampled and transferred to the GPU. With knowledge of graph semantics, data layout, and operator-specific schedules, Pigeon can help improve the scheduling of sampling and data transfer, and generate CUDA kernels at the beginning of propagation that gather data from the host memory on the fly [20].

Develop Pigeon into a full-fledged RGNN compiler that co-designs computation and data. We plan to complete the code generator so that it can generate code for common RGNN operators without intervention. On top of that, we plan to devise new sparse adjacency encoding schemes to enable data reuse from both the source node and destination node during traversal, thus removing the bottleneck in the memory bandwidth that single-sided reuse cannot. Besides, as another integral component in the design space, we seek insights in designing intermediate data layout.

7 Conclusion

RGNN execution has performance challenges due to the inherent computation pattern, the gap between the programming interface and kernel APIs, and the high kernel optimization cost due to its coupling with layout and heterogeneity. To systematically address these performance challenges, we presented the Pigeon IR and code generator for end-to-end RGNN training and inference. The IR design *decouples* the model semantics, data layout, and operator-specific schedule, and *expresses* these opportunities to allow them to be integrated into the design space as integral elements.

By building on one GEMM template and a traversal template, Pigeon already achieves up to $7.8\times$ speed-up in inference and up to $5.6\times$ speed-up in training compared with state-of-the-art systems when executing RGCN, RGAT, HGT on heterogeneous datasets provided by DGL and OGB. We further propose and evaluate two techniques made possible by the Pigeon IR-based code generator, i.e., linear-operator fusion, and compact tensor materialization, and further obtain up to $2.0\times$ speed-up in inference and up to $2.2\times$ speed-up in training compared to the Pigeon unoptimized code.

Acknowledgments

The authors would like to thank anonymous reviewers for their constructive comments. Kun Wu owes thanks to Dr. Seung Won Min and Prof. Guohao Dai for initiating this collaboration, precious advice on GNNs and this project.

References

- [1] Stephan Bloehdorn and York Sure. Kernel Methods for Mining Instance Data in Ontologies. In David Hutchison, Takeo Kanade, Josef Kittler, Jon M. Kleinberg, Friedemann Mattern, John C. Mitchell, Moni Naor, Oscar Nierstrasz, C. Pandu Rangan, Bernhard Steffen, Madhu Sudan, Demetri Terzopoulos, Doug Tygar, Moshe Y. Vardi, Gerhard Weikum, Karl Aberer, Key-Sun Choi, Natasha Noy, Dean Allemang, Kyung-Il Lee, Lyndon Nixon, Jennifer Golbeck, Peter Mika, Diana Maynard, Riichiro Mizoguchi, Guus Schreiber, and Philippe Cudré-Mauroux, editors, *The Semantic Web*, volume 4825, pages 58–71. Springer Berlin Heidelberg, Berlin, Heidelberg, 2007. http://link.springer.com/10.1007/978-3-540-76298-0_5.
- [2] Dan Busbridge, Dane Sherburn, Pietro Cavallo, and Nils Y. Hammerla. Relational graph attention networks. *arXiv preprint arXiv:1904.05811*, 2019. <https://arxiv.org/abs/1904.05811>.
- [3] Tianqi Chen, Thierry Moreau, Ziheng Jiang, Lianmin Zheng, Eddie Yan, Haichen Shen, Meghan Cowan, Leyuan Wang, Yuwei Hu, Luis Ceze, Carlos Guestrin, and Arvind Krishnamurthy. TVM: An Automated End-to-End Optimizing Compiler for Deep Learning. In *13th USENIX Symposium on Operating Systems Design and Implementation (OSDI 18)*, pages 578–594, 2018. <https://www.usenix.org/conference/osdi18/presentation/chen>.
- [4] Victor de Boer, Jan Wielemaker, Judith van Gent, Michiel Hildebrand, Antoine Isaac, Jacco van Ossenberg, and Guus Schreiber. Supporting Linked Data Production for Cultural Heritage Institutes: The Amsterdam Museum Case Study. In David Hutchison, Takeo Kanade, Josef Kittler, Jon M. Kleinberg, Friedemann Mattern, John C. Mitchell, Moni Naor, Oscar Nierstrasz, C. Pandu Rangan, Bernhard Steffen, Madhu Sudan, Demetri Terzopoulos, Doug Tygar, Moshe Y. Vardi, Gerhard Weikum, Elena Simperl, Philipp Ciminiano, Axel Polleres, Oscar Corcho, and Valentina Presutti, editors, *The Semantic Web: Research and Applications*, volume 7295, pages 733–747. Springer Berlin Heidelberg, Berlin, Heidelberg, 2012. http://link.springer.com/10.1007/978-3-642-30284-8_56.
- [5] Gerben K. D. de Vries. A Fast Approximation of the Weisfeiler-Lehman Graph Kernel for RDF Data. In David Hutchison, Takeo Kanade, Josef Kittler, Jon M. Kleinberg, Friedemann Mattern, John C. Mitchell, Moni Naor, Oscar Nierstrasz, C. Pandu Rangan, Bernhard Steffen, Madhu Sudan, Demetri Terzopoulos, Doug Tygar, Moshe Y. Vardi, Gerhard Weikum, Camille Salinesi, Moira C. Norrie, and Óscar Pastor, editors, *Advanced Information Systems Engineering*, volume 7908, pages 606–621. Springer Berlin Heidelberg, Berlin, Heidelberg, 2013. http://link.springer.com/10.1007/978-3-642-40988-2_39.
- [6] Asim Kumar Debnath, Rosa L. Lopez de Compadre, Gargi Debnath, Alan J. Shusterman, and Corwin Hansch. Structure-activity relationship of mutagenic aromatic and heteroaromatic nitro compounds. Correlation with molecular orbital energies and hydrophobicity. *Journal of Medicinal Chemistry*, 34(2):786–797, February 1991. <https://pubs.acs.org/doi/abs/10.1021/jm00106a046>.
- [7] Matthias Fey and Jan Eric Lenssen. Fast graph representation learning with pytorch geometric. *arXiv preprint arXiv:1903.02428*, 2019. <https://arxiv.org/abs/1903.02428>.
- [8] Qiang Fu, Yuede Ji, and H. Howie Huang. TLP-GNN: A Lightweight Two-Level Parallelism Paradigm for Graph Neural Network Computation on GPU. In *Proceedings of the 31st International Symposium on High-Performance Parallel and Distributed Computing, HPDC '22*, pages 122–134, New York, NY, USA, June 2022. Association for Computing Machinery. <https://doi.org/10.1145/3502181.3531467>.
- [9] Yuntao Gui, Yidi Wu, Han Yang, Tatiana Jin, Boyang Li, Qihui Zhou, James Cheng, and Fan Yu. HGL: Accelerating Heterogeneous GNN Training with Holistic Representation and Optimization. In *Proceedings of the International Conference on High Performance Computing, Networking, Storage and Analysis*, pages 1–15, 2022. <https://dl.acm.org/doi/abs/10.5555/3571885.3571980>.
- [10] Mert Hidayetoglu, Carl Pearson, Vikram Sharma Mailthody, Eiman Ebrahimi, Jinjun Xiong, Rakesh Nagi, and Wen-Mei Hwu. At-Scale Sparse Deep Neural Network Inference with Efficient GPU Implementation. <http://arxiv.org/abs/2007.14152>, September 2020.
- [11] Weihua Hu, Matthias Fey, Marinka Zitnik, Yuxiao Dong, Hongyu Ren, Bowen Liu, Michele Catasta, and Jure Leskovec. Open Graph Benchmark: Datasets for Machine Learning on Graphs. <http://arxiv.org/abs/2005.00687>, February 2021.

- [12] Yuwei Hu, Zihao Ye, Minjie Wang, Jiali Yu, Da Zheng, Mu Li, Zheng Zhang, Zhiru Zhang, and Yida Wang. FeatGraph: A Flexible and Efficient Backend for Graph Neural Network Systems. In *SC20: International Conference for High Performance Computing, Networking, Storage and Analysis*, pages 1–13, Atlanta, GA, USA, November 2020. IEEE. <https://ieeexplore.ieee.org/document/9355318/>.
- [13] Ziniu Hu, Yuxiao Dong, Kuansan Wang, and Yizhou Sun. Heterogeneous Graph Transformer. In *Proceedings of The Web Conference 2020*, pages 2704–2710, Taipei Taiwan, April 2020. ACM. <https://dl.acm.org/doi/10.1145/3366423.3380027>.
- [14] Guyue Huang, Guohao Dai, Yu Wang, Yufei Ding, and Yuan Xie. Efficient Sparse Matrix Kernels based on Adaptive Workload-Balancing and Parallel-Reduction. <http://arxiv.org/abs/2106.16064>, October 2021.
- [15] Guyue Huang, Guohao Dai, Yu Wang, and Huazhong Yang. GE-SpMM: General-Purpose Sparse Matrix-Matrix Multiplication on GPUs for Graph Neural Networks. In *SC20: International Conference for High Performance Computing, Networking, Storage and Analysis*, pages 1–12, November 2020. <https://dl.acm.org/doi/10.5555/3433701.3433796>.
- [16] Thomas N Kipf and Max Welling. Semi-supervised classification with graph convolutional networks. *arXiv preprint arXiv:1609.02907*, 2016. <https://arxiv.org/abs/1609.02907>.
- [17] Fredrik Kjolstad, Shoaib Kamil, Stephen Chou, David Lugato, and Saman Amarasinghe. The tensor algebra compiler. *Proceedings of the ACM on Programming Languages*, 1(OOPSLA):1–29, October 2017. <https://dl.acm.org/doi/10.1145/3133901>.
- [18] Chris Lattner, Mehdi Amini, Uday Bondhugula, Albert Cohen, Andy Davis, Jacques Arnaud Pienaar, River Riddle, Tatiana Shpeisman, Nicolas Vasilache, and Oleksandr Zinenko. MLIR: Scaling Compiler Infrastructure for Domain Specific Computation. In *CGO 2021*, 2021. <https://ieeexplore.ieee.org/document/9370308>.
- [19] Wen mei W. Hwu, David B. Kirk, and Izzat El Hajj. *Programming Massively Parallel Processors*. Morgan Kaufmann, fourth edition, 2023. <https://www.sciencedirect.com/book/9780323912310/programming-massively-parallel-processors>.
- [20] Seung Won Min, Kun Wu, Sitao Huang, Mert Hidayetoğlu, Jinjun Xiong, Eiman Ebrahimi, Deming Chen, and Wen-mei Hwu. Large graph convolutional network training with GPU-oriented data communication architecture. *Proceedings of the VLDB Endowment*, 14(11):2087–2100, July 2021. <https://dl.acm.org/doi/10.14778/3476249.3476264>.
- [21] Israt Nisa. [Feature] Gather mm by isratnisa · Pull Request #3641 · dmlc/dgl. <https://github.com/dmlc/dgl/pull/3641>, January 2022.
- [22] Nvidia. Controlling Data Movement to Boost Performance on the NVIDIA Ampere Architecture. <https://developer.nvidia.com/blog/controlling-data-movement-to-boost-performance-on-ampere-architecture/>, September 2020.
- [23] Nvidia. Accelerating Matrix Multiplication with Block Sparse Format and NVIDIA Tensor Cores | NVIDIA Technical Blog. <https://developer.nvidia.com/blog/accelerating-matrix-multiplication-with-block-sparse-format-and-nvidia-tensor-cores/>, March 2021.
- [24] Nvidia. cuBLAS Library User Guide v12.0. <https://docs.nvidia.com/cuda/cublas/index.html>, December 2022.
- [25] Md. Khaledur Rahman, Majedul Haque Sujon, and Ariful Azad. FusedMM: A Unified SDDMM-SpMM Kernel for Graph Embedding and Graph Neural Networks. In *2021 IEEE International Parallel and Distributed Processing Symposium (IPDPS)*, pages 256–266, May 2021. <https://ieeexplore.ieee.org/document/9460486>.
- [26] Michael Schlichtkrull, Thomas N. Kipf, Peter Bloem, Rianne van den Berg, Ivan Titov, and Max Welling. Modeling Relational Data with Graph Convolutional Networks. In Aldo Gangemi, Roberto Navigli, Maria-Esther Vidal, Pascal Hitzler, Raphaël Troncy, Laura Hollink, Anna Tor-dai, and Mehwish Alam, editors, *The Semantic Web*, volume 10843, pages 593–607. Springer International Publishing, Cham, 2018. http://link.springer.com/10.1007/978-3-319-93417-4_38.
- [27] Kristina Toutanova and Danqi Chen. Observed versus latent features for knowledge base and text inference. In *Proceedings of the 3rd Workshop on Continuous Vector Space Models and Their Compositionality*, pages 57–66, Beijing, China, July 2015. Association for Computational Linguistics. <https://aclanthology.org/W15-4007>.
- [28] Minjie Wang, Da Zheng, Zihao Ye, Quan Gan, Mufei Li, Xiang Song, Jinjing Zhou, Chao Ma, Lingfan Yu, Yu Gai, et al. Deep graph library: A graph-centric, highly-performant package for graph neural networks. *arXiv preprint arXiv:1909.01315*, 2019. <https://arxiv.org/abs/1909.01315>.

- [29] Zhaokang Wang, Yunpan Wang, Chunfeng Yuan, Rong Gu, and Yihua Huang. Empirical analysis of performance bottlenecks in graph neural network training and inference with GPUs. *Neurocomputing*, 446:165–191, July 2021. <https://www.sciencedirect.com/science/article/pii/S0925231221003659>.
- [30] Yidi Wu, Kaihao Ma, Zhenkun Cai, Tatiana Jin, Boyang Li, Chenguang Zheng, James Cheng, and Fan Yu. Seastar: Vertex-centric programming for graph neural networks. In *Proceedings of the Sixteenth European Conference on Computer Systems*, pages 359–375, Online Event United Kingdom, April 2021. ACM. <https://dl.acm.org/doi/10.1145/3447786.3456247>.
- [31] Zhiqiang Xie, Minjie Wang, Zihao Ye, Zheng Zhang, and Rui Fan. Graphiler: Optimizing graph neural networks with message passing data flow graph. In D. Marculescu, Y. Chi, and C. Wu, editors, *Proceedings of Machine Learning and Systems*, volume 4, pages 515–528, 2022. <https://proceedings.mlsys.org/paper/2022/file/a87ff679a2f3e71d9181a67b7542122c-Paper.pdf>.
- [32] Zhiqiang Xie and Zihao Ye. Graphiler Repository on Github. <https://github.com/xiezhq-hermann/graphiler>, January 2023.
- [33] Zihao Ye, Ruihang Lai, Junru Shao, Tianqi Chen, and Luis Ceze. SparseTIR: Composable Abstractions for Sparse Compilation in Deep Learning. <http://arxiv.org/abs/2207.04606>, November 2022.
- [34] Da Zheng and George Karypis. The Nature of Graph Neural Network Workloads. <https://hc33.hotchips.org/assets/program/tutorials/HC2021.Amazon.DaZheng.v2.pdf>, August 2021.